Growth and electrical transport of germanium nanowires

G. Gu,[a] M. Burghard, G. T. Kim, G. S. Düsberg, P. W. Chiu, V. Krstic, and S. Roth
Max-Planck-Institut für Festkörperforschung, Heisenbergstrasse 1, D-70569 Stuttgart, Germany

W. Q. Han
Department of Physics, University of California, Berkeley, California 94720-7300

(Received 22 May 2001; accepted for publication 14 August 2001)

Single crystalline germanium nanowires have been synthesized from gold nanoparticles based on a vapor–liquid–solid growth mechanism. Germanium powder was evaporated at 950 °C, and deposited onto gold nanoparticles at 500 °C using argon as a carrier gas. The diameter of the germanium nanowires ranged from 20 to 180 nm when gold thin films were utilized as the substrate, while the nanowires grown from 10 nm Au particles showed a narrower diameter distribution centered at 28 nm. The growth direction of germanium nanowires is along the [111] direction, determined by high resolution transmission electron microscopy. Transport measurements on individual Ge nanowires indicate that the wires are heavily doped during growth and that transport data can be explained by the thermal fluctuation tunneling conduction model. © *2001 American Institute of Physics.* [DOI: 10.1063/1.1413495]

I. INTRODUCTION

Nanostructured materials and devices are important for both fundamental research and applications because they provide a link between molecular and solid state physics, and have the potential to reach far higher device densities compared to traditional semiconductor technology. One kind of nanostructured materials is one-dimensional nanowires and nanotubes, which have been produced by arc discharge,[1–3] laser ablation,[4–6] chemical vapor deposition,[7–14] or chemical transport reactions.[15,16] Much effort has focused on carbon nanotubes due to their interesting electrical properties, such as ballistic conduction at room temperature,[17] and field effect.[18,19] Up to now, no selective growth method for semiconducting carbon nanotubes was available. Semiconductor nanowires can overcome the limitation of selective growth and could be combined with modern semiconductor technology. Based on the vapor–liquid–solid (VLS) growth mechanism, silicon nanowires were synthesized with silane.[20,21] Very recently silicon nanowire devices were fabricated and their transport properties were studied.[22] Germanium nanowires were also prepared by laser ablation using a composite target of germanium and gold.[5] Germanium is one of the important semiconductors which, for example, can be used as a sensitive photodetector in the infrared region. Moreover, the excitonic Bohr radius of bulk (24.3 nm) Ge is larger than that of Si (4.9 nm),[16] hence resulting in more prominent quantum size effects.

In the present article, a simple method based on the VLS mechanism[23] is employed to produce germanium nanowires on supporting gold nanoparticles. Ge nanowires with radii smaller than their Bohr radius and narrow diameter distributions were obtained. Transport measurements on individual Ge nanowires indicate ohmic contacts between Ge nanowires and gold electrodes at room temperature, and that Ge nanowires were heavily doped during synthesis. Electrical transport data are interpreted by the thermal fluctuation tunneling model.

II. EXPERIMENTAL DETAILS

A. Ge nanowire growth

A tube furnace was used for Ge nanowire synthesis. Argon gas with purity of 99.995% was used as a carrier gas to transport germanium clusters produced by evaporation of germanium powder at 950 °C. The pressure of the argon gas was approximately 1.2 bar and the flow rate is approximately 30 standard cubic centimeter per minute (sccm) during growth. Evaporated gold films with 2 nm thickness and 10 nm Au nanoparticles, respectively, on Si/SiO_2 wafers were used as the substrates. The Au thin films were annealed at 500 °C for 30 min in vacuum in order to form Au nanoparticles. Silicon substrates with a silicon dioxide layer of 300 nm were treated with 3-aminopropyl-triethoxysilane (3-APS) solution (6 μl 3-APS in 10 ml H_2O), and the Au nanoparticles (Sigma Inc.) with diameters of 10 nm were deposited onto the substrate. The substrates were placed downstream of the furnace at a temperature of 500 °C for 2 min. The substrates were studied by atomic force microscopy (AFM) with a Nanoscope IIIa system (Digital Instruments) in tapping mode using commercial silicon cantilevers under ambient conditions. Scanning electron microscopy (SEM) images were obtained with a Hitachi S-800 field emission source microscope.

B. Ge nanowire device fabrication

Ge nanowires were dispersed by ultrasonic agitation into an aqueous sodium dodecyl sulfate solution (1 wt %) and deposited on a SiO_2 layer 500 nm thick on a heavily doped

[a]Electronic mail: gang@klizix.mpi-stuttgart.mpg.de

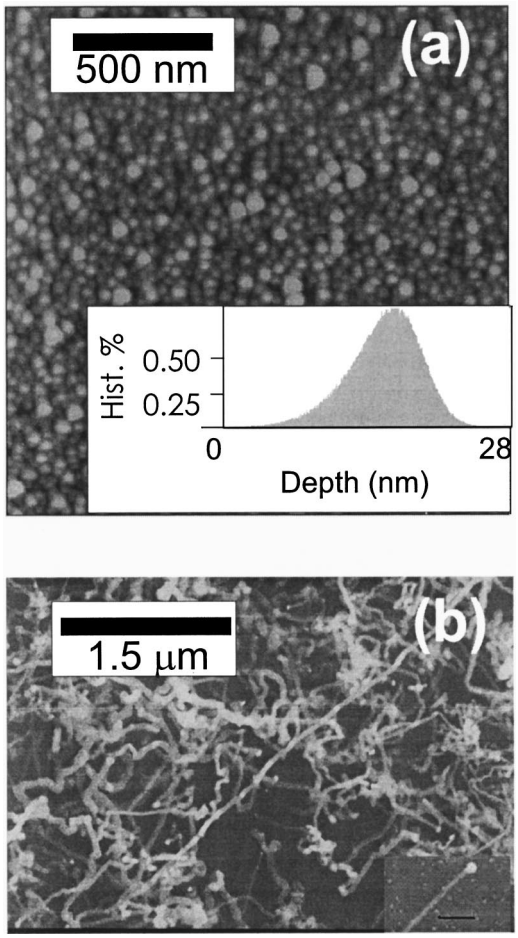

FIG. 1. (a) AFM image of a Au thin film 2 nm thick after annealing. In the inset is the diameter distribution of gold particles, and (b) SEM images of Ge nanowires. The inset shows one nanowire with one nanoparticle at its end (the scale bar for the inset is 200 nm).

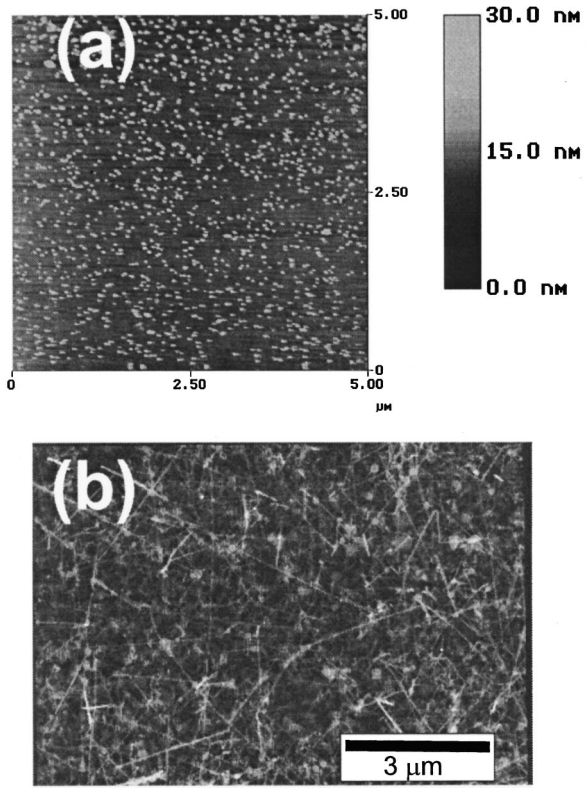

FIG. 2. (a) AFM image of a low density Au nanoparticle on a substrate, and (b) SEM image of Ge nanowires grown from 10 nm Au particles to SEM image of Ge nanowires grown from these low density 10 nm Au particles.

Si wafer, which was used as a back gate. Gold/titanium (175 nm/15 nm thickness) electrodes were prepared by thermal evaporation. The electrodes were separated by a 4 μm gap, which was created by using a thin wire (tungsten, 4 μm diameter) as a shadow mask during evaporation.[24] Transport measurements were performed in a two-terminal configuration under vacuum (10^{-4} mbar). Ge nanowires with diameters of around 100 nm were selected for device fabrication because they can be readily found with optical microscopy.

III. RESULTS AND DISCUSSION

A. Ge nanowires grown on annealed Au thin film

Figure 1(a) shows a typical AFM image of the Au thin film after annealing, showing that the substrate was covered by dense Au nanoparticles with average particle size of 15 nm. After deposition of Ge, the surface of the thin film was found to be covered by a thin, dark brown layer.

A typical SEM image of the Ge nanowires obtained is shown in Fig. 1(b). The image shows that the substrate was homogeneously covered by Ge nanowires, some of which are straight, but slightly curved nanowires are prominent probably due to defects in the nanowires. The diameter of the nanowires falls into the range of 20–180 nm. During nanowire growth, Ge clusters condense at the Au particles, resulting in the growth of droplets of Au–Ge. Ge nanowires, which grow from liquid droplets of Au–Ge due to supersaturation of Ge, show reasonably larger diameters than those of the original Au nanoparticles. The inset of Fig. 1(b) presents one Ge nanowire with one nanoparticle at the end. Energy dispersive x-ray spectroscopy (EDX) revealed that the particle contains Au and a small amount of Ge, supporting the VLS mechanism for Ge nanowire growth.

B. Ge nanowires grown from Au nanoparticles

Ge nanowires were also grown from well-defined Au nanoparticles deposited onto silicon substrates. The Au nanoparticles were homogeneously distributed on the silicon wafer and this was confirmed by our AFM image shown in Fig 2(a). Straight Ge nanowires were obtained, as shown in Fig. 2(b), indicating fewer defects in the nanowires. The average wire diameter is 28 nm. The diameter distribution is from 20 to 45 nm, as determined by transmission electron microscopy (TEM). This range is narrower compared to that grown from Au nanoparticles by annealing Au thin films. This difference may be related to the homogeneous diameter distribution of well-separated Au nanoparticles.

A substrate with a moderately high density of Au nanoparticles [Fig. 3(a)] was used to obtain Ge nanowires of high density. As shown in Fig. 3(b), entangled and pure Ge nanowires with similar diameter distribution were obtained. This indicates that the morphology of Ge nanowires is related to the density of Au nanoparticles on the substrate.

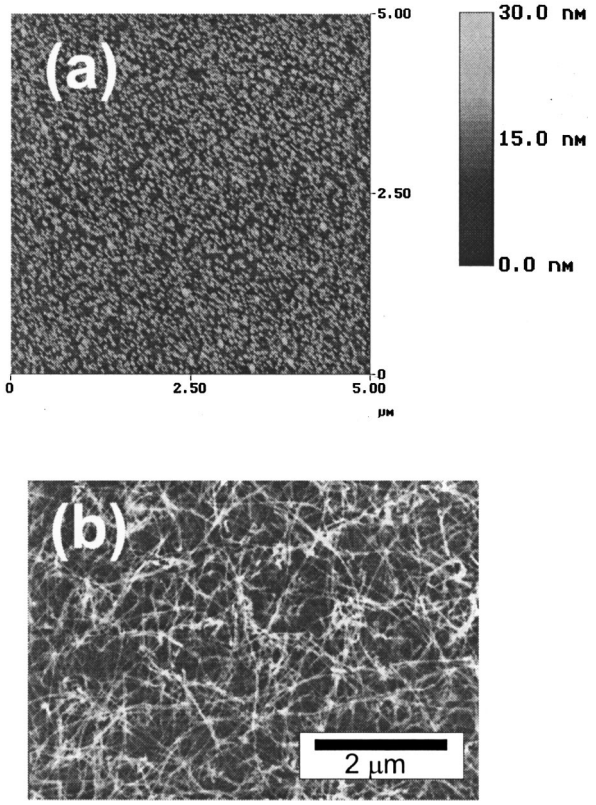

FIG. 3. (a) AFM image of a high density Au nanoparticle on a substrate, and (b) SEM image of Ge nanowires grown from 10 nm Au particles to SEM image of Ge nanowires grown from these high density 10 nm Au particles.

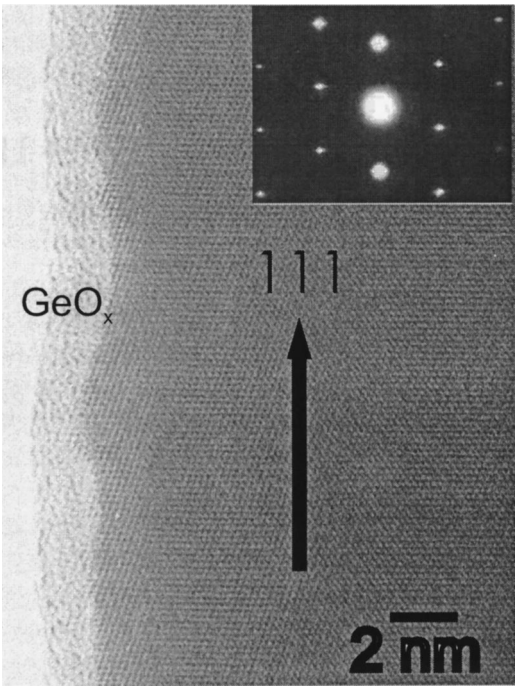

FIG. 4. HRTEM image of a Ge nanowire for which the selected area electron diffraction was recorded along the $\langle 0\bar{1}1 \rangle$ zone axis.

Homogeneous Ge nanowires with radii smaller than 24 nm, the effective Bohr radius, were synthesized from Au nanoparticles.

We also tried to grow Ge nanowires from a higher density of Au nanoparticles, however the diameter distribution of Ge nanowires is broad, similar to the case of annealed Au thin films.

C. Microstructure of Ge nanowires

The nanowires were peeled off, dispersed in acetone, and deposited onto a copper grid coated with an amorphous carbon layer for high resolution transmission electron microscopy (HRTEM) (JEM 400EX, JEOL). A representative HRTEM image is shown in Fig. 4, where the inset is the corresponding electron diffraction pattern. The growth direction of the nanowires is found to be along the [111] direction, the nanowires are well crystallized, and are covered by a 1–2 nm thick layer of amorphous oxide. EDX analysis of individual nanowires showed that they contain only Ge and a small amount of oxygen.

IV. ELECTRICAL TRANSPORT THROUGH INDIVIDUAL Ge NANOWIRES

Typical temperature dependence current–voltage characteristics on a Ge nanowire with diameter of 120 nm are shown in Fig. 5(a) and Fig. 5(b) is a AFM image of a two-terminal Ge nanowire device. At temperatures higher than 100 K linear current dependence on voltage was found, indicating ohmic contacts between the Ge nanowire and the Au electrodes. The Ge nanowires are covered by a thin layer (1–2 nm) of Ge oxide as determined by HRTEM. Germanium oxide is slightly soluble in water and could possibly lead to a thin contact oxide layer and consequently ohmic contact around room temperature. The linear resistivity including contact resistance at room temperature ranged from 1.4×10^{-2} to 30 Ω cm, corresponding to an impurity concentration of at least 10^{16} cm^{-3}.[25] No gate dependence was observed in the Ge nanowires, suggesting that the Ge nanowires were highly doped during growth.

In order to investigate the transport mechanism of the Ge nanowires, temperature dependencies of the linear resistance at small bias voltage were plotted in Fig. 6. Hopping conductivity[26] and photoconductivity[27] were found in gold-doped bulk germanium. However, the resistance data can be fitted well within the framework of the fluctuation-induced tunneling model,[28] where the thermally activated voltage fluctuations across insulating gaps are crucial in the determination of the temperature and electric field dependence of the conductivity. This model has been successfully applied for carbon-polyvinylchloride composites, doped polyacetylene in the metallic regime, and heavily doped, closely compensated for GaAs, and can be described by

$$R = R_0 \exp\left(\frac{T_1}{T+T_0}\right), \tag{1}$$

based on a parabolic barrier approximation, where R is the resistance at different temperatures, T_1 denotes the activation energy at high temperatures, and T_0 is the characteristic temperature around which the most rapid change in the effective barrier height occurs. By fitting the results with Eq. (1), $T_1 = 432$ K and $T_0 = 78$ K was obtained. The Ge nanowire is

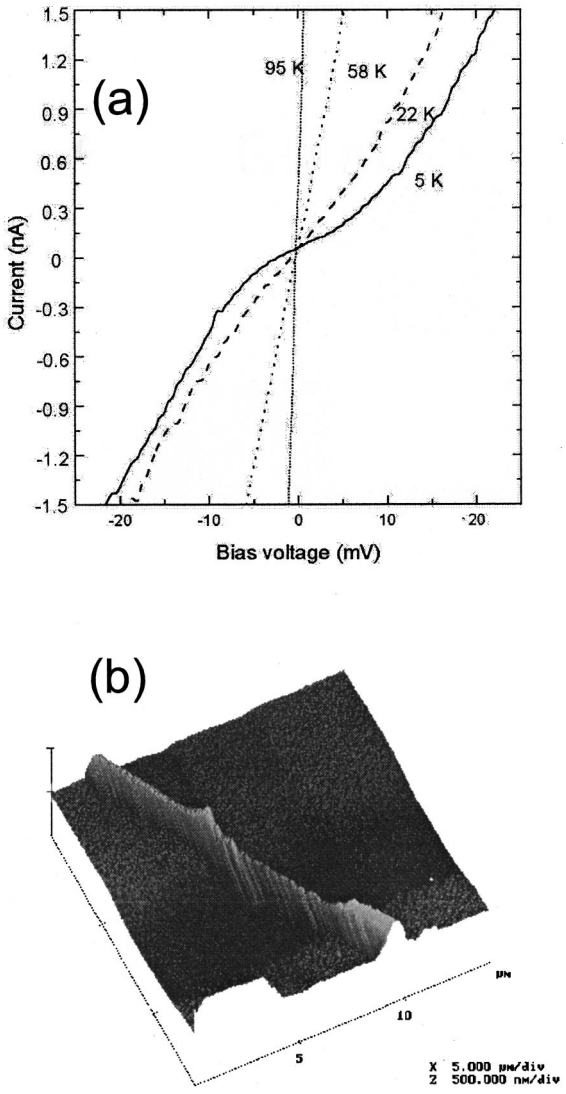

FIG. 5. (a) I–V curves of Ge nanowires at different temperatures, and (b) AFM image of a Ge nanowire device.

similar to heavily doped, closely compensated for, crystalline GaAs considering its low resistivity and heavy doping with Au atoms which can serve as both *p*-type and *n*-type dopants.[29] The nonohmic current–voltage curve at low temperature fits well based on the model and similar T_1 and T_0 values were obtained. T_0 and T_1 are related to the energy barrier V_0 by[28]

$$T_0 = \frac{16\epsilon_0 \hbar A V_0^{3/2}}{\pi e^2 k_B (2m)^{1/2} \omega^2}, \tag{2}$$

$$T_1 = \frac{8\epsilon_0 A V_0^2}{e^2 k_B \omega}, \tag{3}$$

where ω is the width of the junction, A its area, and V_0 the height of its contact potential, k_B is the Boltzmann constant, e the electron charge, m the electron effective mass, and ϵ_0 the vacuum permittivity. If it is assumed that m is the free electron mass and the junction area A is the cross section of the Ge nanowire, the effective junction width and barrier height are estimated to be 4.3 nm and 8 meV, respectively.

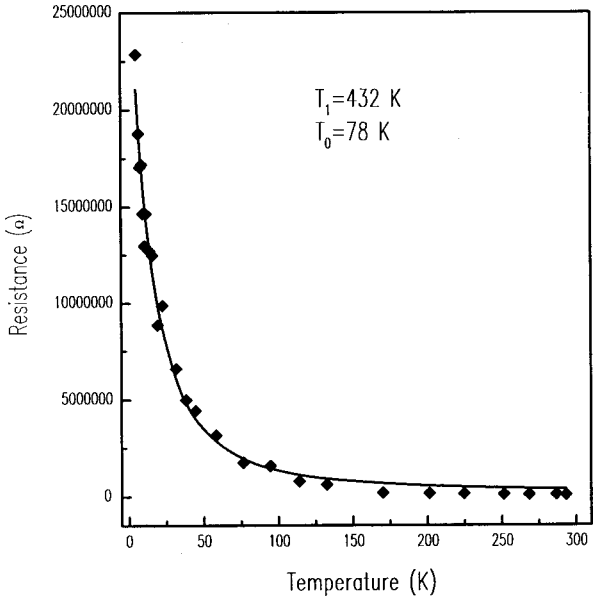

FIG. 6. Linear resistance dependence on the temperature, where diamonds are experimental data and the solid line is the fitting curve according to the thermal fluctuation-induced tunneling model. T_1 and T_0 are the parameters described in Eq. (1).

Assuming that the contact area between the gold electrode and the Ge nanowire is the junction area, a junction width of 11 nm is obtained, which is much larger than the oxide layer of Ge nanowires. Therefore, it is suggested that the potential barriers in the devices more likely result from barriers within the Ge nanowire due to inhomogeneous doping with Au along the nanowire.

The minimum resistivity obtained is 1.4×10^{-2} Ω cm, corresponding to a doping concentration of 2×10^{-3} at. % of Au, however the largest solid solubility of Au in Ge is less than 1.4×10^{-3} at. %.[30] It was reported that the conductivity of doped bulk germanium is very sensitive to its surface states.[31,32] In the case of Ge nanowires surface states may play a more important role due to their high ratio of surface atoms. Si nanowires surface states were suggested to contain a large number of charge carriers.[22] In the Ge nanowire devices reported here, surface states may also contribute to the observed high conductivity. Further experiments are necessary to clarify whether the same is true for the present Ge nanowires.

V. SUMMARY

Based on the vapor–liquid–solid mechanism, Ge nanowires from Au nanoparticles were synthesized. The optimal Au nanoparticle density was found to yield pure Ge nanowires with narrow diameter distributions. The Ge nanowires obtained were well crystallized and growth occurred along the [111] direction. The technique described is simple but effective for the fabrication of Ge nanowires for different applications. Transport measurements on individual Ge nanowires at different temperatures suggest possible roles of fluctuation-induced tunneling in heavily doped Ge nanowires.

ACKNOWLEDGMENTS

Three of the authors would like to thank the Alexander von Humboldt Foundation for support. The authors are grateful to Manfred Schmid, Ulrike Waizmann, Monika Riek, and Thomas Reindl for technical assistance.

[1] S. Iijima, Nature (London) **354**, 56 (1991).
[2] C. Journet, W. K. Maser, P. Bernier, A. Loiseau, M. L. Delachapelle, S. Lefreant, P. Deniard, R. S. Lee, and J. E. Fischer, Nature (London) **388**, 756 (1997).
[3] W. Han, P. Redlich, F. Ernst, and M. Rühle, Appl. Phys. Lett. **76**, 652 (2000).
[4] A. Thess *et al.*, Science **273**, 483 (1996).
[5] A. M. Morales and C. M. Lieber, Science **279**, 208 (1998).
[6] Y. F. Zhang, Y. H. Tang, N. Wang, D. P. Yu, C. S. Lee, I. Bello, and S. T. Lee, Appl. Phys. Lett. **72**, 1835 (1998).
[7] A. M. Cassell, J. A. Raymakers, J. Kong, and H. Dai, J. Phys. Chem. B **103**, 6484 (1999).
[8] E. Flahaut, A. Govindaraj, A. Peigney, Ch. Laurent, A. Rousset, and C. N. R. Rao, Chem. Phys. Lett. **300**, 236 (1999).
[9] I. Willems, Z. Kónys, J.-F. Colomer, G. Van Tendeloo, N. Nagaraju, A. Fonseca, and J. B. Nagy, Chem. Phys. Lett. **317**, 71 (2000).
[10] H. Kind, J.-M. Bonard, C. Emmenegger, L-O. Nilsson, K. Hernadi, E. Maillard-Schaller, L. Schlapbach, L. Forró, and K. Kern, Adv. Mater. **11**, 1285 (1999).
[11] M. Terrones *et al.*, Nature (London) **388**, 52 (1997).
[12] W. Z. Li, S. S. Xie, L. X. Qian, B. H. Chang, B. S. Zou, W. Y. Zhou, R. A. Zhao, and G. Wang Science **274**, 1701 (1996).
[13] Z. F. Ren *et al.*, Appl. Phys. Lett. **75**, 1086 (1999).
[14] T. I. Kamins, R. S. Williams, Y. Chen, Y.-L. Chang, and Y. A. Chang, Appl. Phys. Lett. **76**, 562 (2000).
[15] M. Remskar, Z. Skraba, R. Sanjinés, and F. Lévy, Appl. Phys. Lett. **74**, 3633 (1999).
[16] Y. Wu and P. Yang, Chem. Mater. **12**, 605 (2000).
[17] S. Frank, P. Poncharal, Z. L. Wang, and W. A. de Heer, Science **280**, 1744 (1998).
[18] S. J. Tans, M. H. Devoret, H. Dai, A. Thess, R. S. Smalley, L. J. Geerings, and C. Dekker, Nature (London) **386**, 474 (1997).
[19] D. H. Cobden, M. Bockrath, P. L. McEuen, A. G. Rinzler, and R. E. Smalley, Phys. Rev. Lett. **81**, 681 (1998).
[20] J. Westwater, D. P. Gosain, S. Tomiya, S. Usui, and H. Ruda, J. Vac. Sci. Technol. B **15**, 554 (1997).
[21] J. Hu, M. Ouyang, P. Yang, and C. M. Lieber, Nature (London) **399**, 48 (1999).
[22] J. Y. Yu, S. W. Chung, and J. R. Heath, J. Phys. Chem. B **104**, 11864 (2000).
[23] R. S. Wagner and W. C. Ellis, Appl. Phys. Lett. **4**, 89 (1964).
[24] P. J. de Pablo, E. Graugnard, B. Walsh, R. P. Andres, S. Datta, and R. Reifenberger, Appl. Phys. Lett. **74**, 323 (1999).
[25] S. M. Sze, *Physics of Semiconductor Devices* (Wiley, New York, 1981).
[26] X. X. Wang, M. Getaneh, C. J. Martoff, and E. Kaczanowicz, J. Appl. Phys. **85**, 8274 (1999).
[27] B. I. Beglov, Y. S. Khariono, and S. G. Yudin, Sov. Phys. Semicond. **3**, 242 (1969).
[28] P. Sheng, Phys. Rev. B **21**, 2180 (1980).
[29] W. C. Dunlap, Phys. Rev. **100**, 1629 (1955).
[30] T. B. Massalski, *Binary Alloy Phase Diagrams* (American Society for Metals, Metals Park, OH, 1986).
[31] E. N. Clarke, Phys. Rev. **99**, 1899 (1955).
[32] R. H. Kingston, Phys. Rev. **98**, 1766 (1955).